The Abdus Salam
International Centre for Theoretical Physics

United Nations
Educational, Scientific and
Cultural Organization

IAEA
International Atomic Energy Agency

1965-38

9th Workshop on Three-Dimensional Modelling of Seismic Waves Generation, Propagation and their Inversion

22 September - 4 October, 2008

Interaction between two subducting plates under Tokyo and its possible effects on seismic hazards.

Francis T. Wu
Department of Geological Science
State University of New York
Binghamton
New York
USA

francis@binghamton.edu

GEOPHYSICAL RESEARCH LETTERS, VOL. 34, L18301, doi:10.1029/2007GL030763, 2007

Interaction between two subducting plates under Tokyo and its possible effects on seismic hazards

Francis Wu,[1] David Okaya,[2] Hiroshi Sato,[3] and Naoshi Hirata[3]

Received 22 May 2007; revised 23 July 2007; accepted 7 August 2007; published 18 September 2007.

[1] Underneath metropolitan Tokyo the Philippine Sea plate (PHS) subducts to the north on top of the westward subducting Pacific plate (PAC). New, relatively high-resolution tomography images the PHS as a well-defined subduction zone under western Kanto Plain. As PAC shoals under eastern Kanto, the PHS lithosphere is being thrusted into an increasingly tighter space of the PAC-Eurasian mantle wedge. As a result, zones of enhanced seismicity appear under eastern Kanto at the top of PHS, internal to PHS and also at its contact with PAC. These zones are located at depths greater than the causative fault of the disastrous 1923 Great Tokyo "megathrust" earthquake, in the vicinity of several well-located historical, damaging (M6 and M7) earthquakes. Thus a rather unique interaction between subducting plates under Tokyo may account for additional seismic hazards in metropolitan Tokyo.
Citation: Wu, F., D. Okaya, H. Sato, and N. Hirata (2007), Interaction between two subducting plates under Tokyo and its possible effects on seismic hazards, *Geophys. Res. Lett.*, *34*, L18301, doi:10.1029/2007GL030763.

1. Introduction

[2] The Kanto region of eastern Japan which surrounds metropolitan Tokyo has been hit by disastrous M $\sim$ 8 and numerous intensely damaging M $\sim$ 7 earthquakes throughout recorded history [*Utsu*, 2006; *Japan Meteorological Agency* (*JMA*), 2006]. Causing more than 100,000 fatalities, the Great Kanto earthquake of 1923 serves as a reminder to the severity of these events [*Takemura*, 2003]. Recent geophysical studies in Japan have confirmed and refined the subsurface geometry under Tokyo of the causative fault of the 1923 M8 earthquake and confirmed it as the megathrust at the interface of the Philippine Sea (PHS) and the Eurasian plates (EUR) [*Ishida*, 1992; *Ohmi and Hurukawa*, 1996; *Ohmi and Hori*, 2000; *Matsubara et al.*, 2005]; based on this model the government of Japan issued in 2005 a long term forecast that a M $\sim$ 7 earthquake has a 70% probability to occur within 30 years in the Kanto region [*Tsumura*, 2005]. Deciphering the seismic hazards of possible future megathrust events requires major effort [*Kobayashi and Koketsu*, 2005; *Tsumura*, 2005]. However, many of the historical M $\sim$ 6–7 earthquakes caused significant damage [*Utsu*, 2006; *JMA*, 2006] and are located 50–90 km under eastern Kanto (Figure 1). The depths of these events preclude their direct association with the megathrust and at present their tectonic origins are not known. To formulate a realistic and comprehensive seismic hazard reduction plan for metropolitan Tokyo and Kanto an understanding is necessary of the generating mechanisms of these events in a broader framework involving the PHS, Pacific (PAC) and EUR tectonic plates.

[3] In terms of plate tectonics, the setting under Kanto is rather unique: the westward-subducting PAC encounters on its top side the northwestward subducting PHS along the Sagami-Suruga-Nankai trough (Figures 1 and 2) [*Seno et al.*, 1993; *Huchon and Labaume*, 1989; *Mazzotti et al.*, 2001]. Although globally not common, isolated cases exist where subducting plates come into contact, for example, in Espanola [*Dolan et al.*, 1998] and in Ontong-Java [*Mann and Taira*, 2004]; but the interaction of PHS and PAC under Kanto is clearly more extensive and better delineated [*Noguchi*, 1998; *Sekiguchi*, 2001; *Sato et al.*, 2005]. The PHS moved in a northerly direction until about 2 my ago [*Seno and Maruyama*, 1984] or as recent as 1 my [*Yamaji*, 2000] when it changed to a WNW direction. As a part of PHS the buoyant Izu-Bonin volcanic arc was transported northward 17–2 my ago to collide with and indent Honshu to form the Izu collision zone, a process that affects the current tectonics of the Kanto Plain. At present PHS moves at a rate of about 30 mm/yr in the NW direction under the Kanto area and about 40 mm/yr toward WNW in Tokai whereas PAC subducts westward at about 10 cm/yr [*Seno and Maruyama*, 1984]. Three-dimensional seismicity shown in Figure 2 and in the auxiliary material reveals the 3-D general plate geometry under Kanto.[1] Although some of the features have been observed in previous works [*Ishida*, 1992; *Matsubara et al.*, 2005; *Kamiya and Kobayashi*, 2007] (see online materials for some comments on the models), when combined with high-resolution tomography significantly different interpretations emerge. In the course of our study we recognize four distinct provinces of the PHS subduction system in the region, from east to west (Figure 1): (A) collision (slab impingement) between PHS and PAC, (B) simple PHS subduction, (C) collision of Izu-Bonin arc with EUR and ill-defined subduction in Izu and the area to its north, and (D) shallow PHS subduction in the eastern Tokai area. In this report we will discuss the details of plate interactions in Zones A and B; relevant information on Zones C and D are included in the auxiliary material.

2. Tomography and Relocation of Earthquakes

[4] To unravel the plate interactions in Zones A and B and identify possible seismogenic structures, well resolved

[1]Department of Geological Sciences, Binghamton University, Binghamton, New York, USA.
[2]Department of Earth Sciences, University of Southern California, Los Angeles, California, USA.
[3]Earthquake Research Institute, University of Tokyo, Tokyo, Japan.

0094-8276/07/2007GL030763$05.00

[1]Auxiliary materials are available in the HTML. doi:10.1029/2007GL030763.

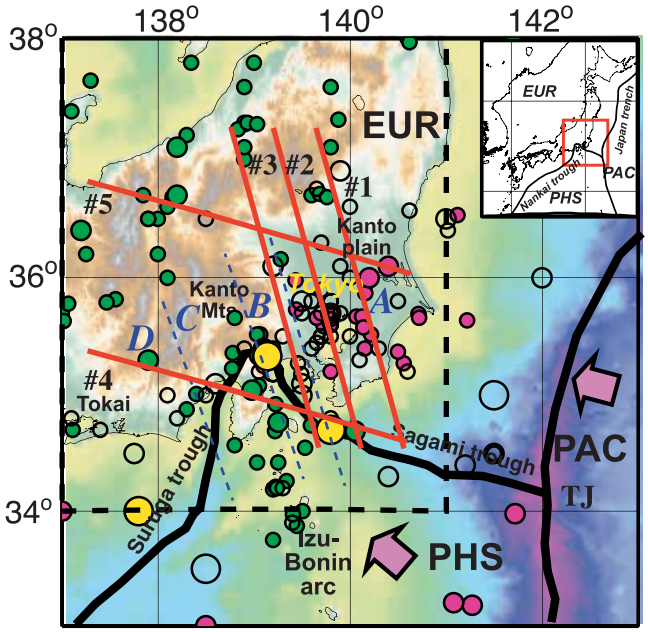

Figure 1. Plate configuration and historical seismicity in Kanto region of central Japan. Philippine Sea (PHS) and Pacific (PAC) plates subduct under Eurasia (EUR) at ~3–4 and ~10 cm/yr, respectively, in directions indicated by arrows. TJ indicates location of EUR-PHS-PAC triple junction. Damaging historical seismicity during 1600–2006 shown as circles. Circle diameters indicate earthquake magnitude: large = M8, medium = M7, small = M6. Circle colors indicate type of earthquake; yellow = megathrust, green = crustal, magenta = sub-crustal. Open circles denote no depth information or the type was not determined. Black dashed box indicates region of seismic tomography and earthquake relocation analyses. Red solid lines are locations of cross-sections shown in Figure 3. A–D are PHS slab zones shown in Figures 2–4. Inset: Location of Figure 1 within central Japan.

patterns of seismicity and seismic velocity anomalies associated with PHS subduction are necessary. Fortunately, the recent densification of Japanese national and regional seismic networks and the wide use of deep (>2 km) borehole and ocean bottom seismic sensors have improved the quantity and quality of seismic phase data for local, shallow and intermediate earthquakes under Kanto. Using P-wave arrival times in the Japan Meteorological Agency (JMA) unified catalog [*JMA*, 2006] as well as its routine hypocentral locations based on an average 1-D velocity model, we iterate tomographic inversion and hypocenter relocation to obtain a 3-D model and new event locations based on the new model. We use an algorithm by *Benz et al.* [1996] for inversion and relocation; the algorithm is particularly appropriate in the Kanto area where the crust and mantle are expected to have rapid velocity variations. Details regarding the tomography and results of resolution tests can be found in the auxiliary material. To assist our interpretation we also obtained a catalog of preliminary focal mechanisms from the *National Research Institute for Earth Science and Disaster Prevention* (*NIED*) [2007].

[5] After viewing the 3-D volumes of tomographic Vp and dVp (differences between the final velocities and the velocities in the initial 1-D model) together with seismicity and focal mechanisms (for M > 4.0), we chose 5 representative profiles to illustrate the main features of the PHS and PAC subduction zones and their interactions. The locations of all five profiles (#1–#5) are shown in Figure 1. Three are approximately north–south in orientation, nearly in the down-dip direction of PHS in Zones A (#1 and #2) and B (#3), and Vp, dVp, and seismicity along them are shown in Figure 3. Profiles #4 and #5 are nearly E–W along-strike across Zones A through D. We should note that in Figure 3 the grey regions at the bottom of the profiles are below the deepest earthquakes used and therefore are not sampled by seismic rays from the source to the stations; other localized smaller grey regions are not resolved simply because they are not well sampled by the rays.

3. Discussion

[6] PHS and PAC can readily be distinguished in the crust as well as in the upper mantle based on Vp and dVp in conjunction with seismicity (Figures 2–3 and auxiliary material). The PAC underlies the entire region and is identified by its characteristic double-seismic zone [*Hasegawa et al.*, 1978] and a mildly positive dVp (<1%). It dips toward the west (Figure 2 and Figure 3 Profiles #4–5) and forms a

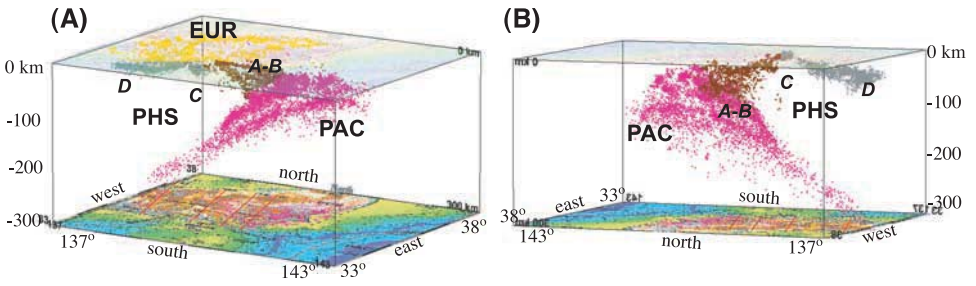

Figure 2. Perspective views of Kanto 3-D seismicity. Views are from (a) south–southeast and (b) north–northwest; full azimuthal coverage available in the auxiliary material movie files. EUR and PAC earthquakes in yellow and magenta dots, respectively. PHS earthquakes shown as brown dots for zones A–B and grey dots for Zone D. See text for zones A–D. Earthquake locations shown in map on block floor and in the auxiliary material. PAC slab dips towards west and has a well-developed double seismic zone. In Figure 2b the EUR earthquakes are removed and the view direction looks up the hinge of the PHS arch related to Izu-Bonin arc; the subducted part of this hinge is seismically quiescent (Zone C). Note that eastern Zone A (brown) portion of PHS interacts with PAC.

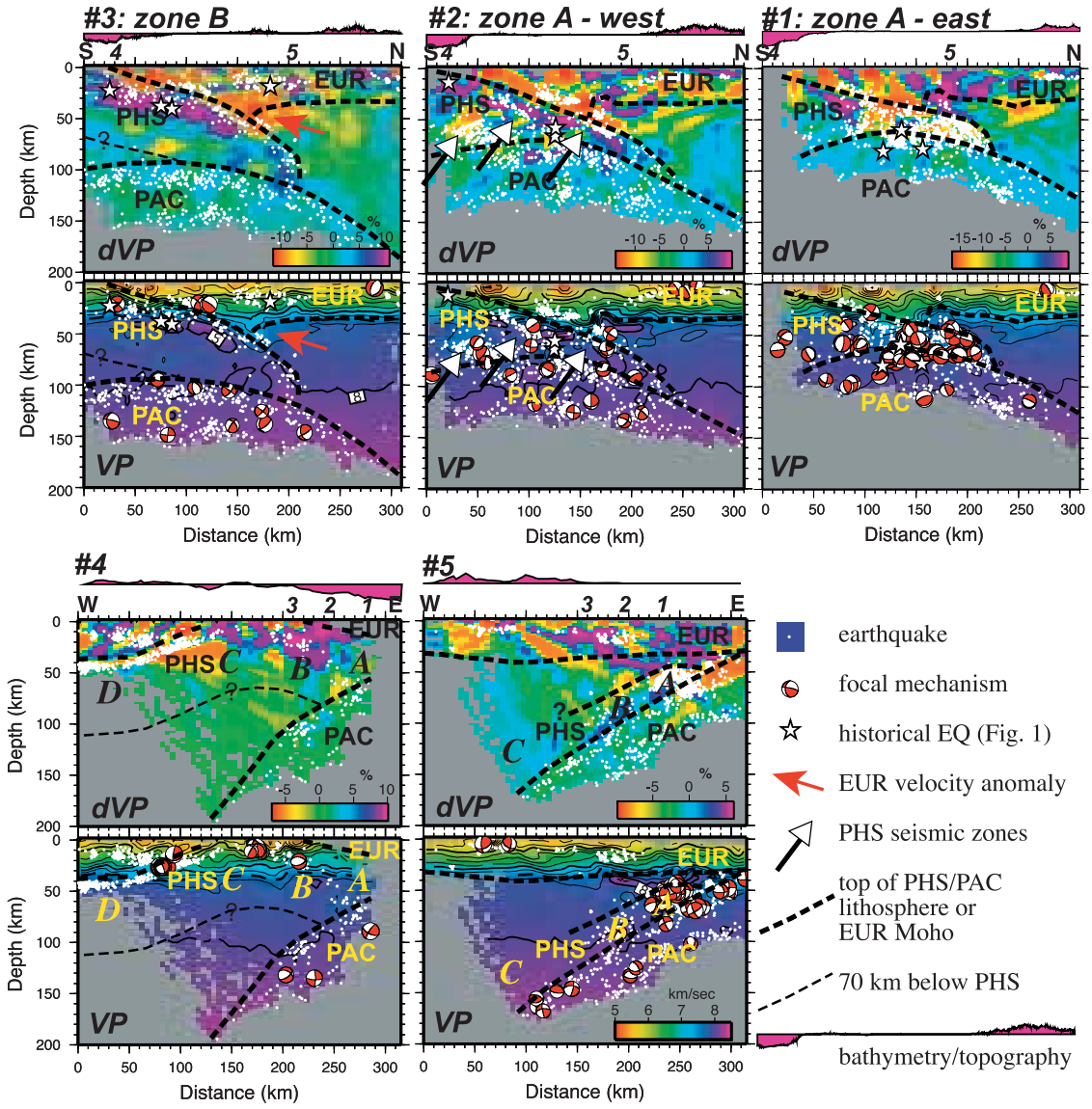

Figure 3. Tomographic cross-sections with superimposed seismicity. Profiles #1–3 are approx. north–south and are dip sections to zones A–B; Profiles #4–5 are east–west; locations shown in Figure 1. For each profile, the upper panel is %dVp relative to starting 1D velocity model [*Ukawa et al.*, 1984] and the lower panel is Vp in km/sec; color scales are in lower right. Topography or bathymetry drawn above panels; numbers denote profile intersections. #1 and #2: Zone A: Enhanced PHS seismicity above PAC double seismic zone. Arrows in #2 show zones of seismicity. #3: Zone B: Subducting PHS whose toe hits PAC. Note PAC double seismic zone. Tectonic erosion of EUR due to PHS subduction (red arrow). #4: Arched PHS interacting with PAC. Subsurface locations of zones A–D labeled. #5: Western quiescent PHS (C); eastern PHS toe (B) and edge (A) interacts with subducting PAC.

mantle wedge with the overlying EUR [*Seno et al.*, 1993]. The PAC is structurally arched in the north–south direction (Figure 3 Profiles #1–3) even as it descends beneath Kanto; this arching is most probably associated with the dynamics of the EUR-PHS-PAC triple junction based on its geometry and location with respect to the plate junction (Figure 1).

[7] PHS is a much more complex structure. It can be traced as a high velocity (dVp ~ +5%) zone dipping to the north in Profile #3 (Figure 3), with seismicity below its upper surface; it represents Zone B in Figures 2 and 3. The intensely studied PHS megathrust zone [e.g., *Kobayashi and Koketsu*, 2005; *Sato et al.*, 2005] is located at shallow depths in this profile. Immediately on top of the PHS, at 30–50 km depth, EUR appears as a prominent low-velocity anomaly (dVp ~ −7%); the thickest part of this anomaly is located where PHS enters the upper mantle (red arrow in Profile #3), implying either accretionary sediments and/or the lower crust of EUR are being carried downward in the subduction process. PHS continues into the upper mantle and impinges onto the top of PAC at the depth of 110–120 km (Profile #3); with thickness of the PHS lithosphere estimated to be about 70 km [*Pacanovsky et al.*, 1999] (marked by a thin dashed line in Figure 3) it must fill much of the space above PAC. To the east of Profile #3, in Zone A, PHS encounters PAC at shallower depths as it is inserted into an increasingly more restricted space capped by EUR

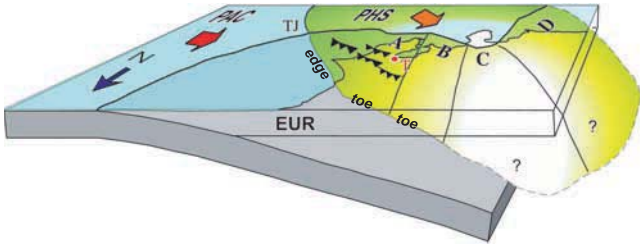

Figure 4. Conceptual model of PHS-PAC-EUR plate configuration. View from northwest. TJ is location of PAC-PHS-EUR triple junction. Red T and dot denote city of Tokyo. A–D are zones of different seismic velocity and seismicity character as defined in text. PHS Zone B toe and Zone A toe and eastern edge interact with PAC. Elevated seismicity and internal deformation exist within Zone A.

(Profile #1 and #2 in Figure 3), compared to that in Profile #3. Concomitantly, its seismicity increased rather noticeably [*Okada and Kasahara*, 1990]; instead of one dipping seismic zone seen in Profile #3 three are found in Profile #2 and in #1 the level of seismicity is noticeably higher. Furthermore, near the contact of PHS the seismicity in PAC is quite high. The shape of the PAC/EUR wedge can be seen in the EW-oriented Profile #5 (Figure 3), nearly parallel to the PAC subduction direction and close to the northern limit of the subducting PHS; here, we see the "toe" of PHS lying on top of PAC. These different patterns of Vp-dVp anomalies and seismicity within Zones A and B exist in even greater contrast to those in zones C and D farther to the west; zone C is seismically quiescent whereas Zone D exhibits seismicity associated with Tokai subduction (Profile #4; see auxiliary material for more details).

[8] The high resolution imaging of the subduction zones allows us to more clearly decipher the relations between the PHS and PAC subduction systems. In Figure 4 we summarize the observations in a schematic plate tectonic model that embodies the processes identified in the crust and upper mantle under Kanto. The along-strike characteristics of the PHS subduction can be divided into the four zones (A–D) as mentioned earlier. Going from west to east in the region under discussion slab-slab plate interaction intensifies. PHS subducts essentially freely in the Tokai area (Zone D) with its Wadati-Benioff zone extending to 70–80 km (see auxiliary material). There are some signs that dipping high Vp velocity anomalies continue beyond this dipping seismic zone. In the Izu Bonin area (Zone C), the collision of the Izu-Bonin arc with EUR is accompanied with the obduction of arc upper crust to form Izu Peninsula. If PHS subduction does take place here it is not clearly expressed either in terms of a dipping seismic zone in the upper mantle or a continuous positive velocity anomaly. But recent seismic imaging profiles indicate shallow thrust faulting possibly associated with PHS subduction [*Sato et al.*, 2005]. The lack of a Wadati-Benioff zone in this area (Figure 3 Profile #4) can perhaps be explained by the elevated thermal state in the zone due to subduction of the Izu-Bonin arc-related volcanic ridge.

[9] However, in Zone B, a clear expression of PHS subduction can be traced from the upper crust into the upper mantle as a bending zone of seismicity and +dVp of about 5%. This zone has typical megathrust structure at shallow levels [*Sato et al.*, 2005] but because its slab toe begins to engage PAC an elevated level of seismicity develops updip within its slab as well. In Zone A, PHS encounters PAC at fairly shallow depths (50–70 km) in the wedge between EUR and PAC. The subduction of PHS is hindered when PHS collides with PAC such that resulting stresses accumulated in PHS lead to intraplate deformation. The closer to the tip of the wedge the more severe is this internal deformation. At the same time, when the toe of PHS hits the relatively fast moving PAC it is subjected to a large shear at the interface. The EUR/PAC mantle wedge is probably thermally cool because of the subduction of cold PHS forearc materials; seismicity is enhanced as a result.

[10] Focal mechanisms of the earthquakes in the constricted area are distinctive from those of others in the region. While the PAC events are dominated by the well-known down-dip compression for the top zone and down-dip tension for the bottom zone [*Hasegawa et al.*, 1978] (Figure 3) the focal mechanisms for the PHS events are more complex. In Zone B (Figure 3 Profile #3) typical interplate shallow-thrust faulting is found for the shallow crustal events; in the upper mantle the available mechanisms indicate down-dip compression. In Zone A (Figure 3 Profiles #1–2) however, in addition to the interplate-type of events – a thrust with one of the planes nearly parallel to the seismic zone – there are more complex patterns of mechanisms (e.g., thrust, normal, strike-slip, as indicated by an arrow in Figure 3 Profiles #1–2) resulting from slab-slab plate interactions.

[11] The model above describes the subduction of PHS, the PHS/PAC interactions and the broad contact of PHS with PAC creates resistance to its advancement. Increased seismicity in Zone A is a result of the intense intraplate deformation of PHS as it is being squeezed within the narrow end of the wedge-shaped space between EUR and PAC. These earthquakes could occur down-dip from the megathrust along the PHS/EUR interface, internal to PHS slab or at locations when PHS engages PAC. The dimensions of the planar seismic zones shown in Figure 3 Profile #2 are on the order of a few tens of kilometers. If one of these zones breaks during one seismic episode, then earthquakes in the M6 and M7 could be generated [*Wells and Coppersmith*, 1994]. From the proximity of the historical hypocenters to zones where plate interaction is taking place (Figure 3, profiles #1 and #2), we propose that these zones may have produced many of the historical M6 and M7 events (Figure 1). More focused studies of finer scale velocity structures, seismicity and focal mechanisms with locally densified arrays as well as the geomechanical behavior of interacting tectonic plates are needed to identify potential rupture surfaces. Future comprehensive estimations of seismic hazards for urban Tokyo must take into account the diverse types of PHS earthquakes due to plate tectonics-driven slab-slab interaction with PAC in addition to the top-of-PHS megathrust earthquakes.

[12] **Acknowledgments.** We thank the Japan Meteorological Agency and the National Research Institute for Earth Science and Disaster Prevention for earthquake catalogues and derived information used in this study. We also thank Hiroko Hagiwara for fruitful discussions. F.W. and D.O. acknowledge partial support provided by the National Science Foundation (USA). H.S. and N.H. acknowledge support provided by the Special Project

for Earthquake Disaster Mitigation in Urban Areas from the Ministry of Education, Culture, Sports, Science and Technology of Japan.

References

Benz, H., B. Chouet, P. Dawson, J. Lahr, and R. Page (1996), Three-dimensional *P* and *S* wave velocity structure of Redoubt Volcano, Alaska, *J. Geophys. Res.*, *101*, 8111–8128.

Dolan, J., H. Mullins, and D. Wald (1998), Active tectonics of the north-central Caribbean: Oblique collision, strain partitioning, and opposing subducted slabs, in *Active Strike-Slip and Collisional Tectonics of the Northern Caribbean Plate Boundary Zone*, edited by J. Dolan and P. Mann, *Spec. Pap. Geol. Soc. Am.*, *326*, 1–62.

Hasegawa, A., N. Umino, and A. Takagi (1978), Double-planed structure of the deep seismic zone in the northeastern Japan arc, *Tectonophysics*, *47*, 43–58.

Huchon, P., and P. Labaume (1989), Central Japan triple junction: A three dimensional compression model, *Tectonophysics*, *160*, 117–133.

Ishida, M. (1992), Geometry and relative motion of the Philippine Sea plate and Pacific plate beneath the Kanto-Tokai district, Japan, *J. Geophys. Res.*, *97*, 489–513.

Japan Meteorological Agency (JMA) (2006), JMA intensity database search for historical earthquake information and data retrieval site (in Japanese), http://www.seisvol.kishou.go.jp/eq/shindo_db/shindo_index.html, Jpn. Meteorol. Agency, Tokyo.

Kamiya, S., and Y. Kobayashi (2007), l Thickness variation of the descending Philippine Sea slab and its relationship to volcanism beneath the Kanto-Tokai district, central Japan, *J. Geophys. Res.*, *112*, B06302, doi:10.1029/2005JB004219.

Kobayashi, K., and K. Koketsu (2005), Source process of the 1923 Kanto earthquake inferred from historical geodetic, teleseismic, and strong motion data, *Earth Planets Space*, *57*, 261–270.

Mann, P., and A. Taira (2004), Global tectonic significance of the Solomon Islands and Ontong Java Plateau convergent zone, *Tectonophysics*, *389*, 137–190.

Matsubara, M., H. Hayashi, K. Obara, and K. Kasahara (2005), Low-velocity oceanic crust at the top of the Philippine Sea and Pacific plates beneath the Kanto region, central Japan, imaged by seismic tomography, *J. Geophys. Res.*, *110*, B12304, doi:10.1029/2005JB003673.

Mazzotti, S., P. Henry, and X. Le Pichon (2001), Transient and permanent deformation of central Japan estimated by GPS, 2. Strain partitioning and arc-arc collision, *Earth Planet. Sci. Lett.*, *184*, 455–469.

National Research Institute for Earth Science and Disaster Prevention (NIED) (2007), Catalogue of focal mechanisms, http://www.bosai.go.jp, Tsukuba, Japan.

Noguchi, S. (1998), Seismicity, focal mechanisms and location of volcanic front associated with the subducting Philippine Sea and Pacific plates beneath the Kanto district, Japan, *Bull. Earthquake Res. Inst. Univ. Tokyo*, *73*, 73–101.

Ohmi, S., and S. Hori (2000), Seismic wave conversion near the upper boundary of the Pacific plate beneath the Kanto district, Japan, *Geophys. J. Int.*, *141*, doi:10.1046/j.1365246X.2000.00086.x.

Ohmi, S., and N. Hurukawa (1996), Detection of the subducting crust of oceanic plates beneath the Kanto district, Japan, *Tectonophysics*, *261*, 249–276.

Okada, Y., and K. Kasahara (1990), Earthquake of 1987, off Chiba, central Japan and possible triggering of eastern Tokyo earthquake of 1988, *Tectonophysics*, *172*, 351–364.

Pacanovsky, K. M., D. Davis, R. Richardson, and D. Coblentz (1999), Intraplate stresses and plate-driving forces in the Philippine Sea Plate, *J. Geophy. Res.*, *104*, 1095–1110.

Sato, H., et al. (2005), Earthquake source fault beneath Tokyo, *Science*, *309*, 462–464.

Sekiguchi, S. (2001), A new configuration and aseismic slab of the descending Philippine Sea plate revealed by seismic tomography, *Tectonphysics*, *341*, 19–32.

Seno, T., and S. Maruyama (1984), Paleogeographic reconstruction and origin of the Philippine Sea, *Tectonophysics*, *102*, 53–84.

Seno, T., S. Stein, and A. E. Gripp (1993), A model for the motion of the Philippine Sea plate consistent with NUVEL-1 and geological data, *J. Geophys. Res.*, *98*, 17,941–17,948.

Takemura, M. (2003), *Great Kanto Earthquake*, Kajima, Tokyo, Japan.

Tsumura, K. (2005), *National Seismic Hazard Maps for Japan*, 162 pp., Earthquake Res. Comm. of the Minist. of Educ. Cult. Sports Sci. and Technol. of Jpn., Tokyo, Japan.

Ukawa, M., M. Ishida, S. Matsumura, and K. Kasahara (1984), A location method for the seismographic network in Kanto and Tokai region, *Res. Notes Nat. Res. Cent. Disaster Prev.*, *51*, 1–88.

Utsu, T. (2006), Catalogue of damaging earthquakes in the world: Ancient times to 2002, ''Utsu-WEQ'', http://iisee.kenken.go.jp/utsu/index.html, Int. Inst. of Seismol. and Earthquake Eng., Tsukuba, Japan.

Wells, D. L., and K. J. Coppersmith (1994), New empirical relationships among magnitude, rupture length, rupture width, rupture area and surface displacement, *Bull. Seismol. Soc. Am.*, *84*, 974–1002.

Yamaji, A. (2000), The multiple inverse method applied to meso-scale faults in mid-Quaternary fore-arc sediments near the triple trench junction off central Japan, *J. Struct. Geol.*, *22*, 429–440.

N. Hirata and H. Sato, Earthquake Research Institute, University of Tokyo, Tokyo 113-0032, Japan. (hirata@eri.u-tokyo.ac.jp; satow@eri.u-tokyo.ac.jp)

D. Okaya, Department of Earth Sciences, University of Southern California, Los Angeles, CA 90089-0740, USA. (okaya@usc.edu)

F. Wu, Department of Geological Sciences, Binghamton University, P.O. Box 6000, Binghamton, NY 13902-6000, USA. (francis@binghamton.edu)